ELSEVIER

Biochimica et Biophysica Acta 1513 (2001) 185–192

BIOCHIMICA ET BIOPHYSICA ACTA
BBA

www.bba-direct.com

Comparison of gramicidin A and gramicidin M channel conductance dispersities

Jeffrey C. Markham [a], Joseph A. Gowen [a], Timothy A. Cross [b], David D. Busath [a,*]

[a] *Department of Zoology and Center for Neuroscience, Brigham Young University, Provo, UT 84602, USA*

[b] *Center for Interdisciplinary Magnetic Resonance at the National High Magnetic Field Laboratory, Institute of Molecular Biophysics and Department of Chemistry, Florida State University, Tallahassee, FL 32306, USA*

Received 17 November 2000; received in revised form 8 May 2001; accepted 10 May 2001

Abstract

To explore the possible role of Trp side chains in gramicidin channel conductance dispersity, we studied the dispersity of gramicidin M (gM), a gramicidin variant in which all four tryptophan residues are replaced with phenylalanine residues, and its enantiomer, gramicidin M^- (gM^-), and compared them to that of gramicidin A (gA). The conductances of highly purified gM and gM^- were studied in alkali metal solutions at a variety of concentrations and voltages, in seven different types of lipid, and in the presence of detergent. Like gA channels, the most common gM channel conductance forms a narrow band. However, unlike gA channels, where the remaining 5–30% of channel conductances are broadly distributed below (and slightly above) the main band, in gM there is a narrow secondary band with $< 50\%$ of the main peak conductance. This secondary peak was prominent in NaCl and KCl, but significantly diminished in CsCl and RbCl. Under some conditions, minor components can be observed with conductances yet lower than the secondary peak. Interconversions between the primary conductance state and these yet lower conductance states were observed. The current–voltage relations for both primary and secondary gM channel types have about the same curvature. The mean lifetime of the secondary channel type is below one third that of the primary type. The variants represent state deviations in the peptide or adjacent lipid structure.

Keywords: Gramicidin; Substate conductance; Mini channel; Multiple conductance state; Current–voltage relationship; State change

1. Introduction

Gramicidin A (gA) channel conductances are distributed into a main gaussian, or 'standard' peak and a broadly distributed subpopulation referred to as 'minis' [1]. gA minis are not variants of primary sequence, secondary structure, or location in the bilayer [2]. They have slightly shorter lifetimes and some appear to interconvert with other mini or standard states, the most common event being between a very low conductance mini (approx. 10% of standard) and a standard state [1,2]. Their single channel current–voltage (iV) relationships are rectifying [1] and have shapes consistent with increased ion binding affinity in the entry on one side of the channel

Abbreviations: gA, gramicidin A; gM, gramicidin M; gM^-, gramicidin M^-; GMO, glycerolmonoolein; GML, glycerolmonolinolein; DPhPC, diphytanoylphosphatidylcholine; DOPC, dioleoylphosphatidylcholine; POPC, Palmitoyloleoylphosphatidylcholine; DOPE, dioleoylphosphatidylethanolamine; POPE, palmitoyloleoylphosphatidylethanolamine; *g*, conductance; *i*, single channel current

* Corresponding author. Fax: +1-801-378-7423.

E-mail address: david_busath@byu.edu (David D. Busath).

0005-2736/01/$ – see front matter
PII: S0005-2736(01)00353-4

according to the three-barrier, two-site, two-ion kinetic model [3]. The low conductance mini iV in asymmetric solutions detected using Na^+ conductance typically has reduced conductance for Cs^+, normal conductance for Ag^+, and increased conductance for H^+, though Na^+ minis with decreased H^+ conductance are also frequently observed [3]. Mini frequency varies from lab to lab [4] and can be modulated by the addition of detergents [5] suggesting that environmental factors may induce the mini state.

One theory for the cause of the minis postulates that the reduced conductance is caused by a change in the dipole due to rotation of a tryptophan to an alternative position. Interactions with the lipid–water interface could stabilize alternative, abnormal tryptophan rotameric conformations, producing a diverse set of tryptophan rotameric conformers for all eight tryptophans, each individual conformation being too low a percentage of the total to be detected spectroscopically. Of the six canonical tryptophan conformations [6], four are energetically plausible according to molecular mechanics [7]: the standard o1 state, an o2 state that would also produce standard channel conductance, and p1 and i1 states, both of which would be expected to produce minis if they are sufficiently stable.

We have therefore studied minis in gramicidin M (gM) channels, in which all four tryptophans are replaced with phenylalanines. Many studies of single channel conductance of gM and gM^- have been published [8–13] but none have focused on the mini conductance state. This is presumably because, as will be shown here, the minis are of very low conductance, short lifetime, and most clearly form a discrete peak in Na^+ and K^+ solutions.

The gM channels in the dominant conductance state have a much smaller conductance than gA standard channels [8] and dramatically superlinear iVs, which have been interpreted as indicative of an increased barrier to ion translocation through the channel [9]. This is probably due to the loss of the dipole moment of the Trp side chain [14], which, in gA, is oriented with the negative end towards the bilayer center in the dominant conformation [15–18]. The low channel conductance renders the studies done here more difficult, yet they are feasible with standard methods. Careful studies of hybridization by Koeppe and colleagues show that gM forms heterodimers with gA as does the enantiomer gM^- with its analogue gA^-, yielding channels of intermediate conductance. The gA peptide does not form heterodimers with gM^-, nor does gA^- form heterodimers with gM. The circular dichroism spectra for gM and gM^- are consistent with right- and left-handed helices, respectively. It was therefore inferred that the dominant conductance states of both gA and gM channels are produced by right-handed $\beta^{6.3}$-helices [11]. For instance, it seems unlikely that a helix with approx. 8.5 or approx. 4.5 residues per turn could form a stable dimer complex with one having 6.5 residues per turn. Likewise, it would seem unlikely for peptides of one hand or pitch to interconvert abruptly to another backbone structure. It was previously argued on similar grounds that gA mini channels had the same backbone structure as standard channels [2]. Therefore, the gM mini channels we discuss here will also be presumed to have the standard backbone structure.

The Trp side chains are also expected to play a role in orienting the gA channel in the membrane [19] as they appear to do in other peptides [20] and proteins [21]. Replacement of the four Trp side chains with Phe has no dramatic effect on channel stability (gA, gM and Trp/Phe variants have mean channel lifetimes on the order of 1 s) with one exception, $Trp_{11}gM$, which has a significantly shorter mean channel lifetime [14].

We report here that rather than a range of minis spread from approx. 10 to 90% of the standard channel conductance, most gM and gM^- minis fall in a single narrow peak with 34–46% of the standard conductance. These were reduced in frequency in RbCl solution and essentially absent in CsCl solution. A small percentage of gM mini channels had smaller conductances (10–34% of standard, hereafter referred to as low minis). The primary and secondary peaks in the single gM channel current histogram are not significantly altered in different lipids or by the addition of Triton X-100. Interconversions between standards and a low mini state (approx. 25% of standard conductance) were observed. The difference between gA and gM channel conductance distribution suggests that the tryptophan side chains of gA play an

important role for a large portion of the gA minis, and that some additional stable variation in the backbone or the environment can cause minis in gM.

2. Materials and methods

All single channel experiments were performed under the conditions described in Busath et al. [22]. gA was obtained from ICN Pharmaceuticals (Cleveland, OH) and diluted in methanol to 10^{-5} mg/ml. gM was prepared by solid-state synthesis using 9-fluroenylmethoxycarbonyl chemistry on an Applied Biosystems model 430A peptide synthesizer [23]. Triton X-100 was obtained from US Biochemical (Cleveland, OH).

The gM sample was purified using high performance liquid chromatography (HPLC). gM was separated from contaminant peptides with a mixture of 93% methanol and 7% water through an octylsilane column, then diluted in methanol to approx. 10^{-5} mg/ml. In one sample, the gM was recrystallized after HPLC purification. Glycerolmonoolein (GMO) and glycerolmonolinolein (GML) were obtained from Nu Chek Prep (Elysian, MN). Diphytanoylphosphatidylcholine (DPhPC), dioleoylphosphatidylcholine (DOPC), palmitoyloleoylphosphatidylcholine (POPC), dioleoylphosphatidylethanolamine (DOPE), and palmitoyloleoylphosphatidylethanolamine (POPE) were obtained from Avanti Polar-Lipids (Alabaster, AL). GMO and GML were suspended in hexadecane at 50 mg/ml. All PC and PE lipids were mixed with decane at 20 mg/ml, with the exception of DOPC, which was mixed with decane at 50 mg/ml. A sample of gM^- was acquired from F. Heitz [8]. It had the same elution profile as gM (data not shown). Approx. 10–20 pg injections of peptide were added to 2–3 ml salt baths (1 M KCl, 2 M KCl, or 1 M NaCl).

Voltage was applied using Ag-AgCl electrodes and a List Medical (Darmstadt, Germany) Patch Clamp L/M-EPC7, or a Warner Instrument (Hamden, CT) Bilayer Clamp BC-525C. The data were collected using a Macintosh computer with a NI-DAQ data acquisition board (National Instruments, Austin, TX) and IGOR Pro software from Wave Metrics (Lake Oswego, OR).

At least 50 channels were observed for each experiment, and three or more experiments were performed at each condition to confirm results.

Analysis of channel current and lifetime was performed using TAC and TACFit from Bruxton (Seattle, WA). Channels with signal-to-noise (channel conductance to peak-to-peak noise) ratios less than 1 were not analyzed.

3. Results

All peptides used in this report were carefully purified with HPLC. The sample of gM^- coelutes with gM. After purification, the majority of channels observed were standard gM channels, with conductance corresponding to published values for gM [12]. Fig. 1 compares gA and gM single channel current distributions in 1 M KCl, GMO. Whereas the mini channels for gA are spread from approx. 10% of the standard conductance up to the standard conductance, nearly all of the mini channels for gM are located between 30% and 40% of the standard current. Low

Table 1
Comparison of standard channel current (i_S) and mini channel current (i_M) under various conditions

Pept.	Lipid	Salt	V_M (mV)	i_S	i_M	i_M/i_S
gM	GMO	1 M KCl	100	0.61 ± 0.04	0.24 ± 0.05	0.39
gM^-	GMO	1 M KCl	100	0.59 ± 0.05	0.21 ± 0.05	0.36
gM	GMO	1 M KCl	150	1.08 ± 0.02	0.40 ± 0.01	0.37
gM	GMO	1 M KCl/detergent[a]	150	1.04 ± 0.02	0.39 ± 0.01	0.38
gM	GMO	1 M NaCl	200	0.62 ± 0.04	0.21 ± 0.05	0.34
gM	GML	1 M KCl	100	1.03 ± 0.01	0.42 ± 0.01	0.40
gM	DPhPC	1 M KCl	200	0.60 ± 0.01	0.28 ± 0.01	0.46

Channel currents are mean ± S.E.M. (pA).
[a]8 μM Triton X-100.

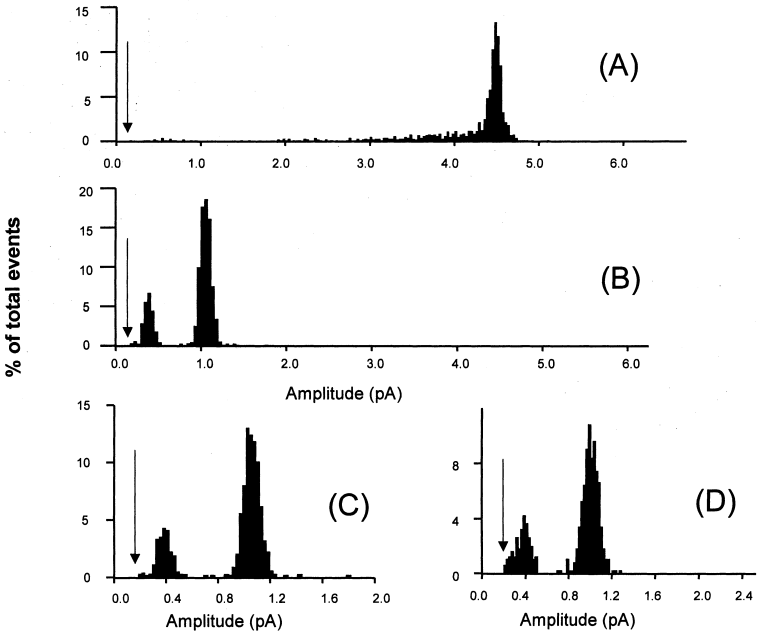

Fig. 1. Comparison of channel types in gA and gM. Histogram of 500+ channels observed in gramicidin A (A) and 200+ channels in gramicidin M on a broad scale (B) and an expanded scale (C), and gramicidin M with 8 μM Triton X-100 in the salt bath (D). Experiments were in 1 M KCl, 100 mV, 21°C (A); 1 M KCl, 150 mV, 21.5°C (B–D) in GMO/hexadecane bilayers. Arrows indicate the threshold determined by baseline noise below which no channels were measured.

minis form the shoulder of the left-hand side of the mini peak. Addition of Triton X-100 did not appear to affect the relative frequency of gM minis (compare Fig. 1C,D). Fig. 2 shows representative examples of various channels observed during an experiment with gM in 1 M KCl. The standard (A), mini (B), and low mini (C) channels are evident in the current traces.

Table 1 shows various conditions under which gM mini channels were observed. For each of the listed conditions, the mean current of the standard channel (i_S) is given. This standard current is then compared to the mean current of the main mini channel type (i_M). The relative current is given by dividing i_M by i_S. The mean mini channel current is consistently 34–46% of the standard channel current, regardless of lipid type (GMO, GML, DPhPC), presence of detergent (Triton X-100), salt bath composition (1 M and 2 M KCl, 1 M NaCl), applied voltage (100–200 mV), and peptide chirality (gM and gM^-). The average frequency of mini channels ranged from 15 to 35% for all of the experimental conditions in Table 1.

The average lifetime of the channels in 1 M KCl, GMO, at 100 mV was 1.34 s for the standard channels and 0.39 s for the mini channels. In all conditions, mini channels appeared to be shorter in average lifetime than corresponding standard channels. Although low minis were quite infrequent, they did not appear to be shorter than standard channels, as exemplified by the low mini arrow C identified in Fig. 2.

Fig. 3 compares current histograms of gM in 1 M KCl (A), 1 M RbCl (B), and 1 M CsCl (C). The lipid and voltage used in A were adjusted so that the standard peak conductance would be comparable to those in B and C. Otherwise, it would have been about half that in C (CsCl), as seen in Table 1, consistent with the K^+/Cs^+ conductance ratio in gA [24].

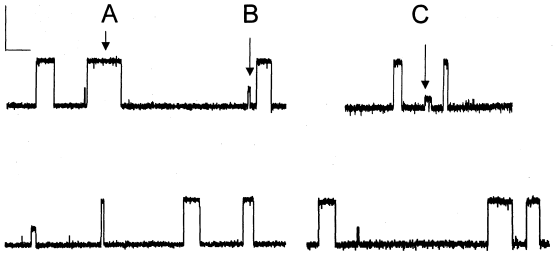

Fig. 2. Single channel current traces of a representative sample of channels observed in gM, 1 M KCl, GMO, 150 mV, 21.5°C. The scale bars represent 1 pA (vertical) and 1 s (horizontal). The arrows point to a standard channel (A), a mini channel (B), and a low mini channel (C).

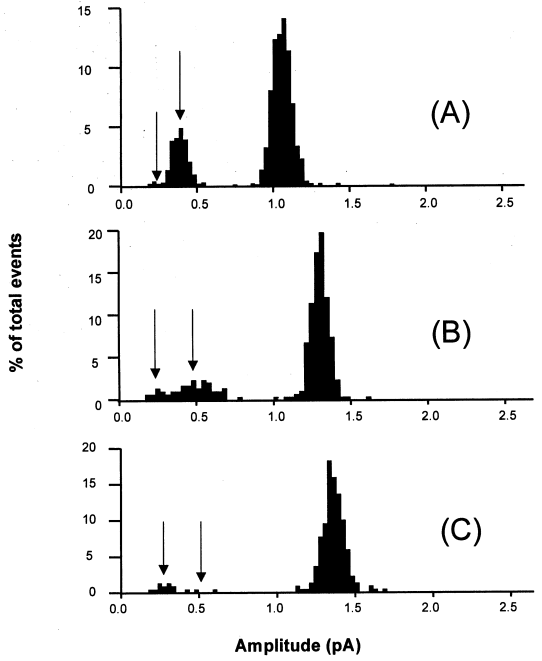

Fig. 3. Current histograms comparing gM conductance dispersities in 1 M KCl (A), 1 M RbCl (B), and 1 M CsCl (C). Each histogram represents 100+ channels observed under the following conditions: GMO/hexadecane, 150 mV, 21.5°C (A); DPhPC/decane, 200 mV, 21.5°C (B); and DPhPC/decane, 200 mV, 21.5°C (C). The mean standard channel conductances are 1.06 ± 0.06 pA (A), 1.30 ± 0.06 pA (B), and 1.37 ± 0.08 pA (C). The left and right arrows designate 22% and 39% of the mean standard channel current, corresponding to the (approximate) relative currents of low mini and mini channels, respectively, in NaCl and KCl solutions.

The discrete mini peak in KCl is reduced in RbCl and nearly absent in CsCl as indicated by the arrows positioned at 22% (representing low minis) and at 39% (representing the secondary peak) of the standard channel conductance in each case. The few variant channels which were observed in CsCl had the relative conductance of low minis.

Fig. 4 shows the current–voltage relationship of the standard (circles) and mini (squares) channels in gM, 1 M KCl, GMO taken from conductance histogram peaks. The current–voltage relations are both superlinear to about the same degree; the g_{200}/g_{100} is 3.13 for the standard channels and 3.03 for the mini channels. Lower voltages were not utilized because of the low conductance of the minis.

Fig. 5 shows some of the observed interconversions between standard and low mini state. We observed four interconversions in 1877 s of channel on-time during 3454 s of data acquisition in 1 M KCl solution, DPhPC/decane bilayers. Three of these are shown in Fig. 5 (traces A and B). One interconversion was seen in 6363 s of channel on-time in GMO, 1 M KCl, 150 mV (data not shown). In the case shown in the first trace, a standard channel converted to a low mini conductance level for a short time (< 100 ms) and then reverted back to standard conductance (Fig. 5A). Fig. 5B shows a two-step turn-on of gM like those observed previously in gA [25] ascribed to an intermediate state in the dimerization process. The presence of two interconversions during a single channel conductance period in Fig. 5A implies beyond doubt these events are not caused by coincidental opening and closing of separate channels. One double interconversion was also observed in CsCl solution (Fig. 5C). In a related set of 1 M KCl experiments designed to study interfacial dipole potential changes several instances of double interconversions were observed, as shown in Fig. 5D. More interconversions were noticed in HCl solutions, but additional conductance peaks were noticed as well, so we chose not to focus on HCl solution properties here.

Because of concern over the role of the lipid or detergents in formation of gA minis, we also checked their effects on the mini conductance peak for gM, as mentioned above. GMO and GML experiments produced similar results. Standard channels in GML

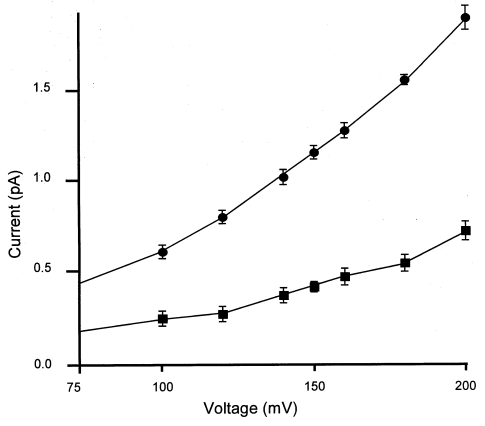

Fig. 4. Current–voltage relationship plot for standard channels (●) and mini (■) channels observed in gM, 1 M KCl, GMO/hexadecane, 100–200 mV, temperature corrected to 23°C. Each point represents the mean current of over 50 channels. The lines extrapolate from the data points at 100 mV toward the point (0,0) on the graph.

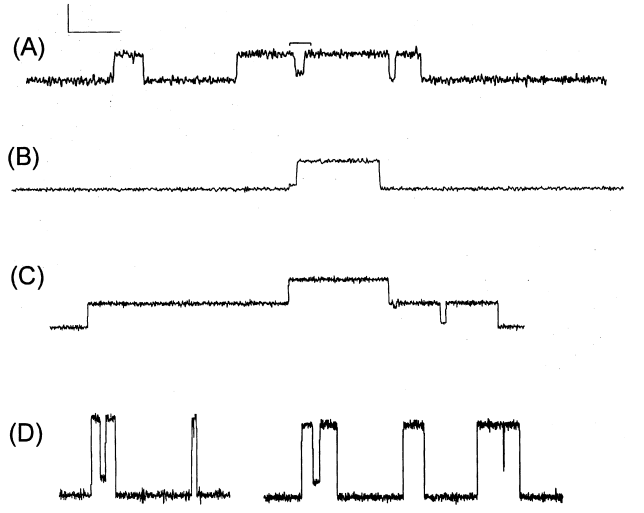

Fig. 5. Interconversions between standard and low mini conductance states of gM channels. Conditions for A and B were DPhPC/decane membrane, 200 mV, 1 M KCl, 21.5°C. In A, the bracket denotes the 100 ms interval during which the standard channel exhibited reduced conductance equivalent to approx. 25% of the standard conductance. In B, a low mini channel converts into a standard channel after 60 ms of on-time. In C, a gM standard converts to a low mini state and then back to a standard state in DPhPC/decane, 200 mV, 1 M CsCl, 21.5°C. In D, there are two examples of standard-to-low mini-to-standard interconversions observed in the same conditions as A and B, but with 1 μg/ml phloretin in the salt bath. The vertical scale bar represents 0.5 pA (A,B,D) or 2 pA (C). The horizontal scale bar represents 500 ms (A,C), 1 s (B), or 2 s (D).

bilayers had about 66% higher current than in GMO bilayers at 100 mV in 1 M KCl (Table 1). The frequencies of mini channels and the i_M/i_S ratios were the same for both lipids, as well as for DPhPC bilayers.

Experiments were also performed in solutions containing 8 μM Triton X-100, similar to gA experiments conducted by Sawyer et al. [5]. Whereas they reported that 8 μM Triton X-100 increased gA mini channel frequency and decreased standard channel conductance, no significant changes in these observables were seen in gM channels with the addition of detergent (Table 1).

In DPhPC bilayers, gM standard channel conductance is reduced compared to GMO and GML bilayers. This is similar to what is found in gA and has been attributed to a greater interfacial dipole potential in phospholipids [22]. Additional experiments were performed in DOPE, POPE, DOPC, and POPC, but the overall channel conductance was too small to accurately assess the mini channel profile. The standard channel mean currents at 23°C are as follows: DOPE, 1 M KCl, 175 mV, 0.33 ± 0.01 pA; POPE, 1 M KCl, 200 mV, 0.34 ± 0.02 pA; DOPC, 1 M KCl, 150 mV, 0.37 ± 0.01 pA; and POPC, 2 M KCl, 150 mV, 0.29 ± 0.01 pA.

4. Discussion

These experiments suggest four main conclusions. First, given the identity of the backbone structures for gM standard and gA standard channels [11], the absence of a broad shoulder of minis (approx. 50–90% of standard current) in gM in all of the conditions indicates that these mini channels in gA are dependent on the presence of the tryptophan side chains.

Second, a phenomenon independent of the tryptophan side chains causes gM to display a well-defined population of mini channels with 34–46% of the standard conductance. Previous studies of gramicidin M present single channel traces and current histograms, although none focus directly on the presence of mini channels. Fonseca et al. [10] and Koeppe et al. [11] present a current histogram and a single channel current trace of gM^- in 1.0 M CsCl, with small numbers of low minis as observed here (Fig. 3C).

Solid state NMR chemical shifts [26] demonstrate that the large monovalent cations bind further from the channel center. Perhaps the optimal binding location of an ion affects its induction of the configuration leading to the secondary conductance state. Hence, Cs^+ almost never induces the mini state, Rb^+ sometimes induces the mini state, and K^+ and Na^+ induce the mini state frequently. It might be noted that another apparently unrelated structural variant of gramicidin A has also been found to display a secondary conductance state [27].

Third, the reduced lifetime of mini gM channels suggests an inherent instability for the mini channels compared to the standard channels. The conformational or configurational change responsible for reducing conductance could also introduce instability to the dimer.

Fourth, the current–voltage relationships for standard and mini channels are superlinear to about the

same degree. Superlinearity in the gM iV has been suggested to be due to a large barrier to passage through the channel such that the most voltage-dependent step is most rate-limiting [9]. If this interpretation is correct, the similarity in iV shape suggests that reduced conductance in the gM mini is not due to an increase in the translocation barrier. Instead, it must be caused either by a distributed retardation throughout each step of the transport process or an increase in energy focused in a fairly voltage-independent region of the reaction coordinate.

Interconversions between the standard and low mini conductance states are observed occasionally in DPhPC bilayers in 1 M KCl at 200 mV. These indicate that gM low minis are conformational or configurational variants of the standard channels rather than peptide contaminants. Fu et al. [28] discovered by solid state NMR that the peptide plane between Val_1 and Gly_2 in gA is rotationally bistable with lifetimes for 10° inward and 20° outward rotational conformations in excess of 10 ms. Perhaps some of the observed states are due to different combinations of these peptide plane-1 rotamers. This seems like an attractive explanation for the observed interconversions. Alternatively, the lipid configuration around the channel could be bistable. So far, no interconversions involving the secondary state have been observed, suggesting that it may represent a more energetically isolated configuration.

One would suppose that the phenomenon responsible for mini channels in gM should also be present in gA. Perhaps the discrete mini peak exists in gA, but is broadened (spread to lower conductances) due to a tryptophan related process, as is the standard peak in the formation of minis with 50–90% on the standard channel conductance. This could partly explain why the sharp peak at 40% of the standard channel conductance is not observed in gA, but it seems more likely that in gA the structural configuration yielding the gM mini peak is not accessible given the total lack of an identifiable secondary peak in the gA conductance histogram.

From these results, one would predict that a more detailed study of the minis found in other gramicidin variants with tryptophans replaced by non-polar side chains, such as gramicidin N (in which the four tryptophan residues of gA are replaced with naphthalalanine residues [29,30]), should reveal the presence of similar mini conductance channels.

It is interesting to note that gA channels also interconvert to a mini state, typically having approx. 10% of the standard channel conductance [2]. Perhaps these interconversions represent similar configurational changes in the two peptides. It may be useful in future studies to explore whether the durations of the gM and gA low mini states derived by interconversion between standard states are consistent with the non-converting mini channel lifetimes. Also, it may be useful to explore our qualitative observation that gM interconversions were more common in DPhPC bilayers at high voltages than in GMO bilayers at low voltages, and that they were more common in H^+ solutions than in alkali metal cation solutions.

In summary, gramicidin M channels are shown to have a discrete secondary permeation state of substantially reduced conductance and lifetime and a low mini state of yet lower conductance. This contrasts with the situation for gramicidin A, which has only one discrete peak with mini conductances forming a disperse shoulder. The additional permeation states for gM imply alternative peptide and/or lipid configurations that are stable on the time scale of seconds.

Acknowledgements

We are grateful to Nathan Bingham, Revell Phillips, and Reed Hendershot, for their initial observations of mini channels in gramicidin M. We also thank Jason Merrell, who performed some of the preliminary single channel experiments, Mark Garrett for single channel current measurements in phloretin-containing solution, and Olaf S. Anderson for helpful discussions. This work is supported by NIH grant AI-23007.

References

[1] D.D. Busath, G. Szabo, Nature 294 (1981) 371–373.
[2] D.D. Busath, G. Szabo, Biophys. J. 53 (1988) 689–695.
[3] D.D. Busath, G. Szabo, Biophys. J. 53 (1988) 697–707.

[4] D.D. Busath, O.S. Andersen, R.E. Koeppe II, Biophys. J. 51 (1987) 79–88.
[5] D.B. Sawyer, R.E. Koeppe II, O.S. Andersen, Biochemistry 28 (1989) 6571–6583.
[6] J.S. Richardson, D.C. Richardson, in: G.D. Fasman (Ed.), Prediction of Protein Structure and the Principles of Protein Conformation, Plenum Press, New York, 1990, pp. 1–98.
[7] A.E. Dorigo, D.G. Anderson, D.D. Busath, Biophys. J. 76 (1999) 1897–1908.
[8] F. Heitz, G. Spach, Y. Trudelle, Biophys. J. 40 (1982) 87–89.
[9] F. Heitz, C. Gavach, G. Spach, Y. Trudelle, Biophys. Chem. 24 (1986) 143–148.
[10] V. Fonseca, P. Daumas, L. Ranjalahy-Rasoloarijao, F. Heitz, R. Lazaro, Y. Trudelle, O.S. Andersen, Biochemistry 31 (1992) 5340–5350.
[11] R.E. Koeppe II, L.L. Providence, D.V. Greathouse, F. Heitz, Y. Trudelle, N. Purdie, O.S. Andersen, Proteins 12 (1992) 49–62.
[12] S.A. Seoh, D.D. Busath, Biophys. J. 68 (1995) 2271–2279.
[13] L.R. Phillips, C.D. Cole, R.J. Hendershot, M. Cotton, T.A. Cross, D.D. Busath, Biophys. J. 77 (1999) 2492–2501.
[14] M.D. Becker, D.V. Greathouse, R.E. Koeppe II, O.S. Andersen, Biochemistry 30 (1991) 8830–8839.
[15] W. Hu, K.C. Lee, T.A. Cross, Biochemistry 32 (1993) 7035–7047.
[16] W. Hu, T.A. Cross, Biochemistry 34 (1995) 14147–14155.
[17] R.E. Koeppe II, J.A. Killian, D.V. Greathouse, Biophys. J. 66 (1994) 14–24.
[18] W. Hu, N.D. Lazo, T.A. Cross, Biochemistry 34 (1995) 14138–14146.
[19] M.R. de Planque, D.V. Greathouse, R.E. Koeppe, H. Schafer, D. Marsh, J.A. Killian, Biochemistry 37 (1998) 9333–9345.
[20] M.R. de Planque, J.A. Kruijtzer, R.M. Liskamp, D. Marsh, D.V. Greathouse, R.E. Koeppe, B. de Kruijff, J.A. Killian, J. Biol. Chem. 274 (1999) 20839–20846.
[21] D.A. Doyle, J. Morais Cabral, R.A. Pfuetzner, A. Kuo, J.M. Gulbis, S.L. Cohen, B.T. Chait, R. MacKinnon, Science 280 (1998) 69–77.
[22] D.D. Busath, C.D. Thulin, R.W. Hendershot, L.R. Phillips, P. Maughan, C.D. Cole, N.C. Bingham, S. Morrison, L.C. Baird, R.J. Hendershot, M. Cotton, T.A. Cross, Biophys. J. 75 (1998) 2830–2844.
[23] M. Cotten, R. Fu, T.A. Cross, Biophys. J. 76 (1999) 1179–1189.
[24] S.B. Hladky, D.A. Haydon, Biochim. Biophys. Acta 274 (1972) 294–312.
[25] F.J. Sigworth, S. Shenkel, Curr. Top. Membr. Transp. 33 (1988) 113–130.
[26] F. Tian, T.A. Cross, J. Mol. Biol. 285 (1999) 1993–2003.
[27] R. Reinhardt, K. Janko, E. Bamberg. in: M. Blank (Ed.), Electrical Double Layer in Biology, Plenum Press, New York, 1986, pp. 91–102.
[28] R. Fu, M. Cotton, T.A. Cross, J. Biomol. NMR 16 (2000) 261–268.
[29] P. Daumas, F. Heitz, L. Ranjalahy-Rasoloarijao, R. Lazaro, Biochimie 71 (1989) 77–81.
[30] L. Ranjalahy-Rasoloarijao, R. Lazaro, P. Daumas, F. Heitz, Int. J. Pept. Protein Res. 33 (1989) 273–280.